Open Phys. 2016; 14:420–425

DE GRUYTER OPEN

Research Article

Open Access

Kalenga Pierre Mubiayi*, Jilian Freitas, Makwena Justice Moloto, Nosipho Moloto, Lucky Mashudu Sikhwivhilu, and Ana Flavia Nogueria

Colloidal synthesis of $CuIn_{0.75}Ga_{0.25}Se_2$ nanoparticles and their photovoltaic performance

DOI 10.1515/phys-2016-0046

Received Aug 30, 2016; accepted Oct 14, 2016

Abstract: This paper addresses the possibilities of synthesizing copper indium gallium selenide nanoparticles with properties that are desired in photovoltaics. The use of oleylamine as solvent and capping agent improved the growth and dispersivity of stoichiometric $CuIn_{0.75}Ga_{0.25}Se_2$ nanoparticles through conventional colloidal synthesis. Relatively small sized $CuIn_{0.75}Ga_{0.25}Se_2$ nanocrystals were assembled in devices as quantum dot sensitized solar cells and exhibited electrical properties with a fill factor of 33% which may be improved for any photovoltaic application.

Keywords: nanoparticles; chalcogenides; devices

PACS: 88. 40 jn; 81.07 Ta; 81.07 Bc; 82.20 Yn

1 Introduction

Copper metal chalcogenides are one of the prominent materials used for photovoltaic applications. The optical, structural and electrical properties of these materials can be tuned in order to overcome the factors currently limiting the improvement of solar cell technology [8, 9, 11, 15, 22, 25]. Copper indium gallium selenide (CIGSe) materials are I-III-VI p-type semiconductors with higher optical absorption coefficients making them beneficial for solar applications [20, 29].

Polycrystalline CIGSe films are mostly prepared by simultaneous or sequential evaporation of the four constituent elements onto the substrate. The film is thus formed in single or multiple steps. This method is more successful and promising when performed under vacuum [14, 26, 28]. Another prevalent technique for film preparation is electrodeposition, consisting of the precipitation of metals from salt-containing electrolyte solutions and their deposition on the cathode surface when the applied potential exceeds the standard reduction potential of the ions. However CIGSe film preparation via this method proves to be very difficult due to the challenge of reaching the desired stoichiometry of the metals from different salts in a common solvent [3, 7, 24]. Much work has been done on bulk CIGSe films possessing the band gap energy between 1.04 and 1.70 eV from which the state-of-the-art fabricated solar cells can achieve 20% efficiency [5, 12, 13, 23]. Recently, researchers have been focusing on the synthesis of nano-sized CIGSe and other quaternary quantum dots with the aim to improve the efficiency of the solar cells beyond 20% and to reduce the cost by using less material. [30] synthesized CISe and CIGSe via a precipitative method. Indium (III) chloride, copper (I) chloride and gallium (III) chloride were heated in a polyol solution in which they were reduced to metal particles. Elemental Se was then added to the solution to form CISe and CIGSe which were then dissolved in ethanol and precipitated by the nucleation process to form the nanocrystals. [10] employed a solvothermal method in which Cu, In, $GaCl_3$, and Se were added to ethylenediamine in an au-

*Corresponding Author: Kalenga Pierre Mubiayi: Department of Chemistry, Faculty of Applied and Computer Science, Vaal University of Technology, Private Bag X021, Vanderbijlpark, 1900, South Africa; Molecular Science Institute, School of Chemistry, University of the Witwatersrand, P. Bag 03, Johannesburg, 2050, South Africa; Email: Kalengam@vut.ac.za

Jilian Freitas: Division of Information displays (DMI), Center for Information Technology Renato Archer (CTI), Campinas, Sao Paulo, Brazil

Makwena Justice Moloto: Department of Chemistry, Faculty of Applied and Computer Science, Vaal University of Technology, Private Bag X021, Vanderbijlpark, 1900, South Africa

Nosipho Moloto: Molecular Science Institute, School of Chemistry, University of the Witwatersrand, P. Bag 03, Johannesburg, 2050, South Africa

Lucky Mashudu Sikhwivhilu: Nanotechnology Innovation Centre, Advanced Materials Division, Mintek, Private Bag X3015, Randburg, 2125, South Africa

Ana Flavia Nogueria: Laboratory of Nanotechnology and Solar Energy, University of Campinas, P.O. Box 6154, 13083-970, Campinas, SP, Brazil

toclave at 230°C for 24 h. A single CIGSe phase was obtained after washing the product with water and drying it at 100°C. Particles with diameters of less than 100 nm were found in strong agglomerations. Although rigorous control is needed, the introduction of defined concentrations of indium and/or gallium in copper selenide might render the semiconducting materials more susceptible to property improvement [2, 6, 18, 22]. Ternary chalcogenides such as CISe can possess a defined stoichiometry but with several crystalline structures where the distribution of copper and indium have different possible orderings [27]. The addition of a Se precursor to oleylamine (OLA) as a capping agent affects the crystal structure of CISe. Sphalerite and chalcopyrite phases were obtained by injection of Se to and along with the mixture of other precursors in OLA [11]. Similar processes can be followed to add one more element, gallium for instance, to CISe in order to obtain a quaternary chalcopyrite material with enhanced properties. [17] employed the arrested precipitative technique to control the addition of Cu to Cd(SSe). $Cu_2Cd(SSe)_2$ crystallites with sizes between 56 and 79 nm were obtained in aggregates and the increase in Cu content favoured the formation of mixed morphologies. Several reports have shown that $CuIn_{0.75}Ga_{0.25}Se_2$ is the stoichiometric CIGSe which may exhibit optimal properties to be exploited for various applications such as solar cells [16, 22, 28].

In this work we report the synthesis of $CuIn_{0.75}Ga_{0.25}Se_2$ via the conventional colloidal method and the study of the dispersivity and reduction of nanoparticle size. We further investigated the possibilities of utilising synthesized nanoparticles in order to improve their properties and photovoltaic capabilities.

2 Experimental

Copper (I) chloride (CuCl, 97%), indium chloride ($InCl_3$, 98%), gallium chloride ($GaCl_3$, 99.99%), selenium powder (Se, 99.99%), TiO_2 (Dyesol), ethane dithiol (EDT, 95%), tri-n-octylphosphine (TOP, 97%), hexadecylamine (HDA, 98%), oleylamine (OLA, 98%), oleic acid (OA, analytical standard), acetonitrile (99.99%), hexane (95%), methanol (99.9%), ethanol (99.9%) and acetone (99.8%) were used as purchased from Sigma Aldrich, South Africa.

2.1 Colloidal synthesis of CIGSe nanoparticles

For a typical synthesis of CIGSe nanoparticles, 6.0 g of HDA was heated in a three-necked flask under argon (Schlenk line). Then 1.0 ml of 1.0 M solution of CuCl in TOP (TOPCuCl), 0.75 ml of 1.0 M $InCl_3$ in TOP ($TOPInCl_3$) and 0.25 ml of 1.0 M $GaCl_3$ in TOP ($TOPGaCl_3$) were added to the solution and the mixture was put under vacuum to remove any air. The resultant solution was heated to 180°C and 1.0 ml of 2.0 M solution of Se in TOP (TOPSe) was then added. The content was heated at 220°C for 30 min. The temperature was then decreased to 60°C. Methanol was then added to the solution to flocculate the nanoparticles and CIGSe nanoparticles were collected after centrifugation. The effect of the solvent on the synthesis of CIGSe was studied.

2.2 Characterization of materials

The optical measurements of the synthesized materials were determined using an Analytica Jena Specord 5D UV-vis Spectrophotometer. The samples were dispersed in toluene and placed in a quartz cuvette. A Perkin Elmer LS45 fluorescence spectrophotometer was used to analyze the photoluminescence of the nanocrystals by dissolving the samples in chloroform and placing them in a quartz cuvette. The structural properties were determined using Bruker a D2 Phaser X-ray diffractometer on crushed samples and the TEM images of nanoparticles were determined using a FEI G^2 Tecnai spirit transmission electron microscope. The FTIR spectra were recorded using a Perkin Elmer 400 spectrometer at room temperature in the wavenumber range of 650 to 4000 cm^{-1}. The thin films and devices were fabricated via ethane dithiol (EDT) treatment following the optimized procedure for CISe as detailed elsewhere [16]. A schematic of the quantum dot sen-

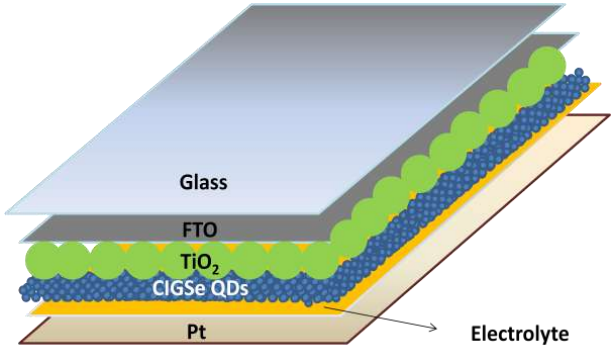

Figure 1: CIGSe QDSSC device.

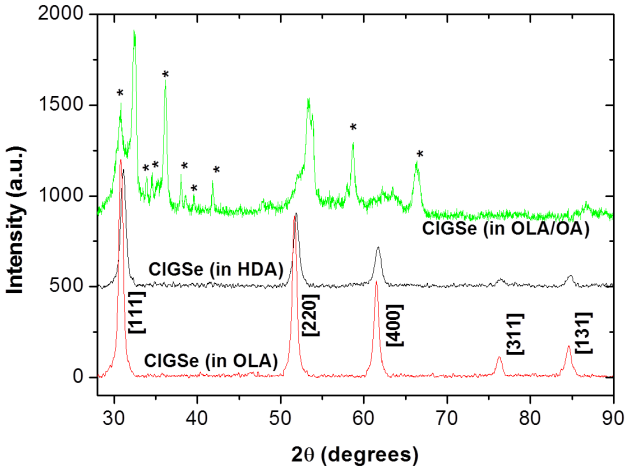

Figure 2: XRD patterns of $CuIn_{0.75}Ga_{0.25}Se_2$ synthesized in HDA, OLA and OLA/OA via CCM. Secondary phases (*) in OLA/OA synthesized CIGSe.

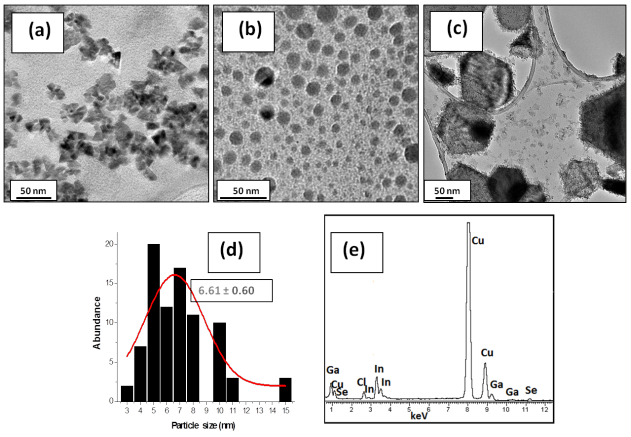

Figure 3: TEM images of $CuIn_{0.75}Ga_{0.25}Se_2$ nanoparticles synthesized via CCM in (a) HDA, (b) OLA and (c) OLA/OLA at 3:1 molar ratio; (e) size distribution and (f) EDS spectrum of $CuIn_{0.75}Ga_{0.25}Se_2$ nanoparticles synthesized in OLA using CCM.

sitized solar cell (QDSSC) device is shown in Fig. 1 below. The surface morphology of the film was determined using a Veeco 3100 SPM atomic force microscope (AFM). The surface image was formed through the deflection of a laser beam focused on a micrometer wide silicon cantilever as it scanned across the CIGSe sample in tapping mode. The optical images of the surface were obtained from an Olympus BX51-P Polarizing optical microscope. The J-V curve was obtained by connecting the FTO and Pt electrodes of the assembled device to an Eco Chemie Autolab PGSTAT 10 potentiostat under standard AM 1.5 conditions using a 150 W Xe lamp as the light source and appropriate filters. The polychromatic light intensity at the electrode position was calibrated to 100 mW cm^{-2} with a silicon photodiode from 1830-C Newport Optical Power Meter.

3 Results and discussion

3.1 Structutal and optical properties of synthesized of CIGSe nanoparticles

The main variable in the synthesis was the solvent. HDA, OLA and a 3:1 ratio of OLA/OA were used as solvents while other parameters were kept constant for synthesis of $CuIn_{0.75}Ga_{0.25}Se_2$. XRD spectra (Fig. 2) showed that the particles synthesized in both OLA and HDA were indexed with tetragonal CIGSe crystalline orientations and confirmed that the particles were nano-sized crystallites. Additional phases were observed when OA was mixed with OLA. This is due to the carboxylic group allowing for different particle growth and crystallinity as different capping sites were created. The secondary peaks may be influenced by the binary or ternary compounds formed as impurities alongside the CIGSe particles.

The nanoparticle morphologies were observed from the TEM coupled with EDS (Fig. 3). The use of HDA as coordinating solvent led to nanoparticles in agglomeration while their synthesis in OLA or OLA/OA gave well dispersed CIGSe. The particle size distribution of $CuIn_{0.75}Ga_{0.25}Se_2$ synthesized in OLA was from about 2 to 20 nm with the average of 6.5 nm (Fig. 3d), showing that the Ostwald ripening effect occurred as the nanoparticles mature from nucleation during the synthesis. OLA/OA favoured the formation of relatively small CIGSe nanoparticles which tended to self-assemble into features with diameters above 50 nm. Nearly pyramidal, spherical and heaxgonal shapes were respectively obtained from HDA, OLA and OLA/OA. This may result in different properties to be utilised in various applications. The size and functional groups of those solvents may play a role in this behaviour. Since the molecular weight of OLA is greater than that of HDA, the vibration and swelling properties of OLA would be less than those form HDA. While the amine group is expected to play a similar role in both HDA and OLA, the particular effect of OLA can be attributed to the double bond giving each OLA the possibility to bend the molecular chain creating a high attraction towards growing particles during synthesis and therefore decreasing the space in which the particles should grow. The EDS analysis proved that copper indium gallium selenide nanoparticles were synthesized. The Carbon (not shown on the graph), chorine and the excess of copper detected here originated

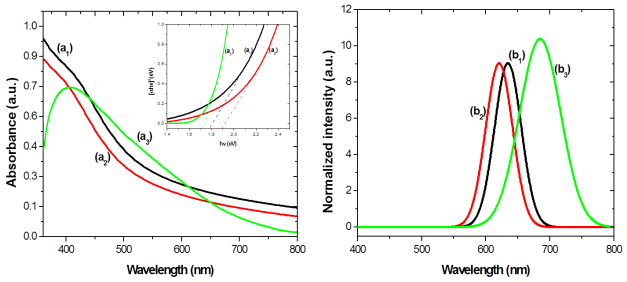

Figure 4: Absorption spectra with the corresponding $(\alpha h\nu)^2$ /hν curves inset and emission spectra of $CuIn_{0.75}Ga_{0.25}Se_2$ nanoparticles synthesized in (a_1, b_1) HDA, (a_2,b_2) OLA and (a_3,b_3) OLA/OA at 3:1 molar ratio.

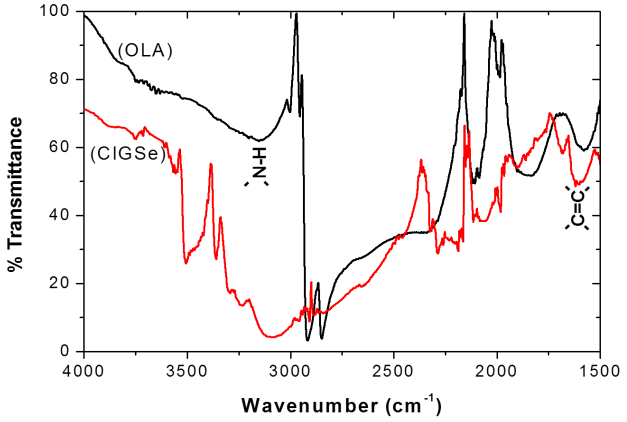

Figure 5: FTIR spectra of CIGSe nanoparticles and pure OLA.

from the copper grid, its lacy carbon, the solvent used to disperse the particles and the ligands adsorbed onto the surface of CIGSe particles. The atomic percentages of Cu, In, Ga and Se were respectively found at 55.9, 24.0, 7.7 and 12.4% while their corresponding theoretical values are 25.2, 18.7, 6.5 and 49.6%. Although the relative atomic percentages could not match with the expected values due to the copper grid used, the Ga and In contents indicated that the expected stoichiometric $CuIn_{0.75}Ga_{0.25}Se_2$ nanoparticles were obtained from the colloidal synthesis. [19] reported similar analysis for the $MoBi_2Se_5$ chalcogenide through EDS. The atomic percentages of Mo, Bi and Se were respectively 12.40, 34.45 and 52.55%. These values relatively matched the theoretical composition of $MoBi_2Se_5$.

The absorption and emission spectra of synthesized CIGSe nanoparticles are shown in Fig. 4. $CuIn_{0.75}Ga_{0.25}Se_2$ prepared in OLA showed pronounced optical characteristics with a band edge and maximum emission peak at 525 and 625 nm respectively as compared to the HDA and OLA/OA counterparts which possessed respectively red-shifted band edges at 550 and 625 nm and maximum emissions at 645 and 685 nm. This is due to the high dispersion and relatively small particle size encountered in the material synthesized in OLA compared to the HDA counterpart. The energy curves (Fig. 4 inset) gave band gaps of 1.72, 1.78 and 1.90 eV respectively for particles synthesized with OLA/OA, HDA and OLA as solvents. The OLA synthesized CIGSe particles had a higher energy gap than those from OLA/OA and HDA syntheses. This confirms the good structural properties as discussed earlier. In other respects, OA brought more competition between the amine and the carboxylic group as responsible for attachment of the ligands to metals.

Furthermore, the presence of carboxylic groups allows for assembly of the formed nanoparticles to yield the hexagonal-like aggregates. Such aggregates could not be observed when OLA was the only coordinating solvent used in the synthesis of CIGSe nanoparticles under the same conditions. Fig. 5 shows a typical FTIR spectrum of OLA synthesized nanoparticles. The main functional groups of OLA, -CH=CH- and $-NH_2$ were also depicted in the CIGSe sample. It may therefore be obvious to confirm that the nanoparticles were indeed formed through OLA as the coordinating agent. The adsorption of solvent molecules onto the surface of the CIGSe nanoparticles was effective. The resulted ligands play a major role for usage of the CIGSe nanoparticles in many applications. This includes the interaction of CIGSe thin film with other layers in solar cell devices.

3.2 Assembly of photovoltaic device

The surface of the CIGSe film was examined by AFM and optical microscope (Fig. 6). The CIGSe film had a roughness that was not consistent throughout the surface of the film. The average roughness was 150 nm and the CIGSe particles could be found agglomerated with the average aggregate size of 200 nm. The film was formed by larger building blocks of CIGSe particles deposited on top of one another and thus creating more grain boundaries that can influence the charge recombination within the device. [21] reported the difference of J/V spectra from grain to grain bringing a high density of defect states at the CIGSe surface. The authors suggested a preferential oxidation of particular grains, which passivated the defect levels at the surface of the film. While this phenomenon could contribute to multiple exciton generation to a certain extent, the charge recombination processes might forbid electrons to move from the active layer to the electrodes and therefore compromise the role of the assembled device as QDSSC.

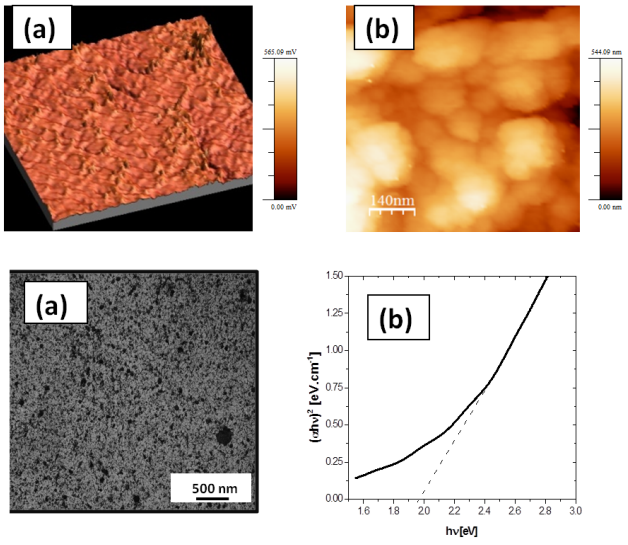

Figure 6: Properties of CIGSe thin film: (a) surface morphology from AFM showing (b) aggregated grains creating grain boundaries; (c) optical microscopic image CIGSe showing some openings within the film and (d) $(\alpha h\nu)^2/h\nu$ curve of CIGSe thin film.

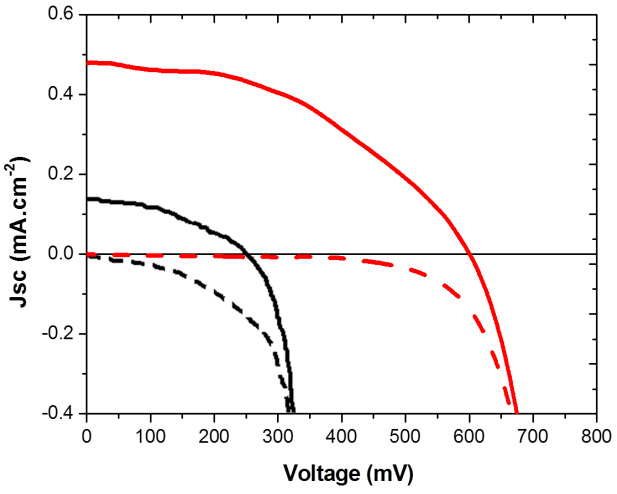

Figure 7: J-V curves of CIGSe QDSSC (black lines) and reference N719 DSC (red lines) devices. Measurements done in the dark (dashed lines) and under AM1.5 illumination (solid lines).

The device assembled as QDSSC from synthesized CIGSe particles showed electrical properties in comparison with the reference N719 dye sensitized solar device fabricated under same the conditions (Fig. 7). The short circuit current density (Jsc) and open circuit voltage (Voc) were 0.168 mA cm^{-2} and of 0.162 V respectively in the QDSSC device. Although a relatively good FF of 33% could be obtained in the assembled device from CIGSe film possessing a band gap energy of 1.93 eV (Fig. 6d), poor electric properties were observed, leading to a very small PCE. Several factors might be held responsible for the poor performance of the device, especially for the fact that the reference N719 showed similar trends, with Voc, Jsc, FF and PCE of 600 mV, 0.471 mA cm^{-2}, 41% and 0.35% respectively. The quality of the film did not favour a good transfer of electrons from the absorber to the wide band gap layer of TiO_2. Although EDT was used as ligand exchange molecules, the attachments of CIGSe particles on the TiO_2 surface could not be optimized. The thickness of the film is also an important parameter in the fabrication of the device. [1] studied the effect of thickness of CdSe film on the properties of a solar cell device. The authors found that increasing the thickness of CuSe film from 548 to 856 nm improved the PCE from 0.27 to 0.62% respectively. The role of the electrolyte could be another consideration as this regenerates the charge in the absorbing layer. The couple I^-/I_3^- should be permanently stable in the device in order for this last to perform better. However the electrolyte could leak anytime within the working conditions.

4 Conclusions

Relatively small sizes of copper indium gallium selenide nanoparticles were obtained through CCM. Monitoring the parameters of synthesis such as the solvent system can allow the formation of well dispersed and relatively small size copper indium gallium selenide nanoparticles with improved optical and structural properties. Despite the poor performance, the trial of device assembly demonstrated that the synthesized $CuIn_{0.75}Ga_{0.25}Se_2$materials possess photovoltaic activities which may further be improved.

Acknowledgement: The authors are thankful to the National Research Foundation (NRF) in South Africa, Vaal University of Technology, University of the Witwatersrand, CTI Renato Archer, CANERGIE and Carsten trust fund for facilities and funding of this project.

References

[1] Bagade C.S., Ghanwat V.B., Khot K.V., Bhosale P.N., Efficient improvement of photo- electrochemical performance of CdSe thin film deposited via arrested precipitation technique, Materials Letters, 2016, 164, 52–55.
[2] Battaglia D., Peng X., Formation of High Quality InP and InAs Nanocrystals in a Noncoordinating Solvent, Nano Letters, 2002, 2, 1027–1030.
[3] Bhattacharya R.N., CIGS-based solar cells prepared from electrodeposited stacked Cu/In/Ga Layers, Journal of the Electro-

chemical Society, 2010, 157, D406–D410.
[4] Contreras M.A., Egaas B., Ramanathan K., Hiltner J., Swartlander A., Hasoon F., et al., Progress toward 20% efficiency in $Cu(In,Ga)Se_2$ polycrystalline thin-film solar cells, Progress in Photovoltaics: Research and Applications, 1999, 7, 311–316.
[5] Contreras, M.A., Ramanathan K., Abushama J., Hasoon F., Young D.L., Egaas B., et al., Short Communication: Accelerated Publication: Diode characteristics in state-of-the-art ZnO/CdS/$Cu(In_1$-xGax$)Se_2$ solar cells, Progress in Photovoltaics: Research and Applications, 2005, 13, 209–216.
[6] Delahoy A.E., Chen L., Akhtar M., Sang B., Guo S., New technologies for CIGS photovoltaics, Solar Energy, 2004, 77, 785–793.
[7] Dini J.W., Electrodeposition, the Materials Science of Coatings and Substrates, Noyes Publications, New York, 1992.
[8] Green M.A., Emery K., King D.L., Hishikawa Y., Warta W., Solar cell efficiency(Version 29), Progress in Photovoltaics: Research and Applications, 2007, 15, 35–40.
[9] Green M.A., Emery K., Hishikawa Y., Warta, W., Solar cell efficiency (Version 29), Progress in Photovoltaics: Research and Applications, 2010, 18, 346–352.
[10] Gu S.I., Shin H.S., Yeo D.H., Hong Y.W., Hahm S., Synthesis of the single phase CIGS particle by solvothermal method for solar cell application, Current Applied Physics, 2011, 11, S99–S102.
[11] Guo Q., Kim S.J., Kar M., Shafarmans W., Birkmire R., Stach E.A., *et al.*, Development of $CuInSe_2$ Nanocrystal and Nanoring Inks for Low-Cost Solar Cells, Nano Letters, 2008, 8, 2982–2987.
[12] Jackson P., Hariskos D., Lotter E., Paetel S., Wuerz R., Menner R., New world record efficiency for $Cu(In,Ga)Se_2$ thin-film solar cells beyond 20%, Progress in Photovoltaics: Research and Applications, 2011, 19, 894–897.
[13] Jager-Waldau A., Progress in chalcopyrite compound semiconductor research for photovoltaic applications and transfer of results into actual solar cell production, Solar Energy Materials & Solar Cells, 2011, 95, 1509–1517.
[14] Kaelin M., Low cost processing of CIGS thin film solar cells. Solar Energy, 2004, 77, 749–756.
[15] Kalenga M.P., Govindraju S., Airo M., Moloto M.J., Sikhwivhilu L.M., Moloto M., Fabrication of a Schottky Device Using CuSe Nanoparticles: Colloidal versus Microwave Digestive Synthesis, Journal of Nanoscience and Nanotechnology, 2014, 14, 1–7.
[16] Kalenga M.P., Synthesis and characterization of copper chalcogenide nanoparticles and their use in solution processed photovoltaics, PhD Thesis, University of the Witwatersrand, Johannesburg, South Africa, 2015, 78–116.
[17] Khot K.V. Mali S.S., Ghanwat V.B., Kharade S.D., Mana R.M. Hong,C.K., *et al.*, Photocurrent enhancement in a $Cu_2Cd(SSe)_2$ photoanode synthesized via an arrested precipitation route, New Journal of Chemistry, 2016, 40, 3277–3288.
[18] Klimov V.L., Mikhailowsky A.A., Xu S., Malko A., Hallingsworth J.A., Leather-dole C.A., Optical gain and stimulated emission in nanocrystal quantum dots, Science, 2000, 290, 314–317.
[19] Mane R.M. Ghanwat, V.B., Kondalkar V.V., Khot K.V., Mane S.R., Patil P.S., et al., Nanocrystalline $MoBi_2Se_5$ Ternary Mixed Metal Chalcogenide Thin-Films for Solar Cell Applications, Procedia Materials Science, 2014, 6, 1285–1291.
[20] Kodigala S.R., $Cu(In_{1-x}Ga_x)Se_2$ based Thin Film Solar Cells. Thin Films and Nanostructures, Vol. 3, Academic Press, Elsevier, San Diego, 2010.
[21] Monig H., Caballero R., Kaufmann C.A., Schmidt, Lux-Steiner M.C., Sadewasser S., Nanoscale investigations of the electronic surface properties of $Cu(In,Ga)Se_2$ thin films by scanning tunneling spectroscopy. Solar Energy Materials & Solar Cells, 2011, 95, 1537–1543.
[22] Panthani M.G. Akhavan V., Goodfellow B., Schmidtke J.P., Dunn L., Dodabalapur A., *et al.*, Synthesis of $CuInS_2$, $CuInSe_2$, and $Cu(In_xGa_{(1-x)})Se_2$ (CIGS) nanocrystal "inks" for printable photovoltaics, Journal of American Chemical Society, 2008, 130, 16770–16777.
[23] Repins I. Contreras M.A., Egaas B., DeHart C., Scharf J., Perkins C.L., *et al.*, 19.8% - efficient ZnO/CdS/$CuInGaSe_2$ solar cell with 81.2% fill factor, Progress in Photovoltaics: Research and Applications, 2008, 16, 235–239.
[24] Saji V.S., Lee S.M., Lee C.W., CIGS thin film solar cells by electrodeposition, Journal of the Korean Electrochemical Society, 2011, 14, 61–70.
[25] Scheer R., Walter, T., Schock H.W., Fearheiley M.L., Lewerenz H.J., $CuInS_2$ based thin film solar cell with 10.2% efficiency, Applied Physics Letters, 1993, 63, 3294–3296.
[26] Schleussner S. Zimmermann U., Watjen T., Leifer K., Edoff M., Effect of gallium grading in $Cu(In,Ga)Se_2$ solar-cell absorbers produced by multi-stage coevaporation, Solar Energy Materials & Solar Cells, 2011, 95, 721–726.
[27] Stanbery B.J., Copper indium selenides and related materials for photovoltaic devices, Critical Reviews in Solid State and Materials Sciences, 2002, 27, 73–117.
[28] Venkatachalam M., Kannan M.D., Muthukumarasamy N., Prasanna S., jayakumar S., Balasundaraprabhu R., *et al.*, Investigations on electron beam evaporated $Cu(In_{0.85}Ga_{0.15})Se_2$ thin film solar cells, Solar Energy, 2009, 83, 1652–1655.
[29] Wallin E., Malm U., Jarmar T., Lundberg O., Edoff M., Stolt L., World-record $Cu(In,Ga)Se_2$-based thin-film sub-module with 17.4% efficiency, Progress in Photovoltaics: Research and Applications, 2012, 20, 851–854.
[30] Wu J.D., Wang L.T., Gau C., Synthesis of $CuInGaSe_2$ nanoparticles by modified polyol route, Solar Energy Materials & Solar Cells, 2012, 98, 404–408.